Effect of Bimetallic Co-Cu/Dolomite Catalyst on Glycerol Conversion to 1,2-Propanediol

Norsahida Azri[1,2,3], Ramli Irmawati[2,3,4]*, Usman Idris Nda-Umar[2,5], Mohd Izham Saiman[2,3], Yun Hin Taufiq-Yap[2,3] and Ghassan Abdulkareem-Alsultan[2,3]

[1]*Preparatory Centre for Science and Technology, Universiti Malaysia Sabah, 88400 Kota Kinabalu, Sabah, Malaysia*
[2]*Department of Chemistry, Faculty of Science, Universiti Putra Malaysia, 43400 UPM, Serdang, Selangor, Malaysia*
[3]*Catalysis Science and Technology Research Centre (PutraCat), Faculty of Science, Universiti Putra Malaysia, 43400 UPM, Serdang, Selangor, Malaysia*
[4]*Laboratory of Processing and Product Development, Institute of Plantation Studies, Universiti Putra Malaysia, 43400 UPM, Serdang, Selangor, Malaysia*
[5]*Department of Chemical Sciences, Federal Polytechnic, PMB 55, Bida, Niger State, Nigeria*

ABSTRACT

This present study examines the efficacy of using dolomite (Dol, $CaMg(CO_3)_2$)-supported copper (Cu) and cobalt (Co) bimetallic and monometallic catalysts for the hydrogenolysis of glycerol to propylene glycol (PG; 1,2-PDO). The proposed catalysts were generated using the impregnation process before they were calcined at 500°C and reduced at 600°C. Advanced analytical techniques namely Brunauer, Emmett, and Teller (BET) method; the Barrett, Joyner, and Halenda (BJH) method; temperature-programmed desorption of ammonia (NH_3–TPD), hydrogen-temperature programmed reduction (H_2-TPR), X-ray diffraction (XRD) analysis, and scanning electron microscopy (SEM) were then used to characterise the synthesised catalysts, whose performance was then tested in the hydrogenolysis of glycerol. Of all the synthesised catalysts tested in the hydrogenolysis process, the Co-Cu/Dol bimetallic catalyst performed best, with an 80.3% glycerol conversion and 85.9% PG selectivity at a pressure of 4 MPa, a temperature of 200°C, and a reaction time of 10 hours. Its high catalytic performance was attributed to effective interactions between its Co-Cu-Dol species, which resulted in acceptable acidity, good reducibility of metal oxide species at low

Norsahida Azri, Ramli Irmawati, Usman Idris Nda-Umar, Mohd Izham Saiman, Yun Hin Taufiq-Yap and Ghassan Abdulkareem-Alsultan

temperatures, larger surface area (15.3 $m^2 g^{-1}$), large-sized particles, fewer pores (0.032 $cm^3 g^{-1}$), and smaller pore diameter (0.615 nm).

Keywords: Cobalt, copper, dolomite support, acidity, glycerol hydrogenolysis, 1,2-propanediol

INTRODUCTION

Glycerol, an important by-product of the biodiesel production process, can be utilised for the production of value-added chemicals such as propylene glycol (PG), which is also called propane-1,2-diol or 1,2-propanediol (1,2-PDO); 1,3-propanediol (1,3-PDO), glycerol carbonates, cyclic acetals/ketals, glycerol esters, glyceric acid, glycerol ethers, acrolein/ acrylic acid, and other speciality chemicals (Liu et al., 2019; Pandhare et al., 2016). Of all these speciality chemicals, PG has a huge market demand owing to its application as a monomer or component in the pharmaceutical industries, as well as a solvent in cosmetics, food, and polyester resins (Gallegos-Suarez et al., 2015; Pudi et al., 2015). The predicted global output of PG is ≈1.4 million tonnes per year, with an annual market growth rate of 4% (Vasiliadou et al., 2011). Traditionally, propylene oxide, generated from various petroleum processing techniques, undergoes the hydration process for synthesising PG (Bagheri et al., 2015; Mallesham et al., 2016; Rajkhowa et al., 2017).

However, as the financial returns from petroleum have decreased and environmental concerns have increased, there are increased efforts to develop a more practical and sustainable method of producing PG. If catalyst-driven hydrogenolysis of glycerol can be successfully developed, it would significantly alter the price of PG due to the benefits of the manufacturing process. According to multiple extant studies, glycerol hydrogenolysis to PG is a dual-step reaction. In the first step, glycerol is converted to acetol by dehydrating it over the catalyst's acidic sites before the resultant acetol is hydrogenated to synthesise PG over the active metallic sites in the catalysts in the second step. The procedure prioritises cleaving the C-O bonds in the glycerol molecules while preventing the cleaving of its C-C bonds to prevent the production of by-products (Zheng et al., 2015).

The hydrogenolysis of glycerol to PG is significantly more efficient with the use of noble-based catalysts, such as platinum (Pt), ruthenium (Ru), palladium (Pd), and cerium (Ce) (Soares et al., 2016; Yu et al., 2010). However, as these catalysts are costly, they are not feasible for industrial applications. Non-noble metal catalysts, such as zinc (Zn), nickel (Ni), copper (Cu), aluminium (Al), iron (Fe), cobalt (Co), and magnesium (Mg) have demonstrated good performance, of which Cu-based catalysts have been used most frequently as they perform best and very efficiently activate the cleaving of C-O bonds instead of C-C bonds (Freitas et al., 2018). Apart from that, Co-based catalysts are also active catalysts that have high PG selectivity (Guo et al., 2009). However, the activity and stability of Cu and Co-based catalysts warrant further investigation to maximise their potential.

As such, bimetallic catalysts are more frequently used as they significantly increase the conversion of glycerol and the selectivity of PG. Bimetallic catalysts are highly effective due to their metal-metal interactions, which enhance their chemical strengths, thermal strengths, acidity, surface area, metallic phase dispersion, and reducibility or oxygen ion mobility (Jiang et al., 2016; Pandhare et al., 2016). More specifically, a catalyst containing Cu, zinc oxide (ZnO), and aluminium oxide (Al_2O_3) was able to completely convert glycerol at a PG selectivity of 80% at a temperature of 240°C and a hydrogen (H_2) pressure of 0.1 MPa (Feng et al., 2011). Meanwhile, a catalyst containing a 1:1 ratio of Cu to Ni as well as Al_2O_3 yielded 89% PG selectivity and converted 60% of the glycerol at a temperature of 210°C and H_2 pressure of 4.5 MPa over a reaction duration of 12 hours (Pudi et al., 2015).

A catalyst containing a 1:3 ratio of Ce to Ni-Co was able to convert 71.3% of the glycerol and select 68.5% of the PG at a temperature of 220°C and a H_2 pressure of 6 MPa over a reaction duration of 10 hours when the glycerol concentration was 20 wt% (Jiang et al., 2016). Similarly, a Cu-Ni/Al_2O_3 catalyst converted 70.5% of the glycerol with a PG selectivity of 70% at 4.5 MPa H_2 pressure, 220°C, and 16-hour reaction duration when the glycerol concentration was 4 wt% (Gandarias et al., 2012). Furthermore, Ru–Cu/Al_2O_3 and Ru–Cu/ZrO_2 catalysts were able to convert 45% and 13.7% of the glycerol and select 94% and 100% of the PG, respectively, using 2.5 H_2 pressure, 200°C, a reaction duration of 24 hours, and a glycerol concentration of 20 wt% (Soares et al.,2016).

During glycerol hydrogenolysis, acid sites and metal surfaces serve dual functions as active reaction sites for dehydration and hydrogenation processes. Therefore, metal-based catalysts with bifunctional sites carry significant potential. These properties enable a catalyst to increase the surface area for depositing the active phase. It also serves as a reservoir for the extra hydrogen molecules that help hydrogenate surface species by enabling hydrogen ions from the dolomite (Dol) support to migrate to the metal particles and create more active sites that are interfacial in the metal support, all of which help increase its catalytic activity (Rajkhowa et al., 2017).

Therefore, this present study prepared three separate Dol-supported Co and Cu catalysts. The Dol support mostly contained magnesium carbonate ($MgCO_3$), calcium carbonate ($CaCO_3$), and varying concentrations of high quantities of ferric oxide (Fe_2O_3), silicon dioxide (SiO_2), and Al_2O_3 that did not exceed 5% w/w. Dolomite (Dol) has grown in popularity as it is cheap and possesses acidic properties. Furthermore, Dol contains Mg and Ca ions, which are well-known as effective reducers for electrochemical series, so Dol may help reduce metal oxides to metallic species. It has also been found to outperform its more conventional, expensive, and time-consuming counterparts, for instance, HZSM-5 zeolites, Mobil® composition of matter no. 41 (MCM-41), Santa Barbara amorphous-15 (SBA-15), and Santa Barbara amorphous-16 (SBA-16) (Vanama et al., 2015).

Dolomite (Dol) is abundantly available and can easily be procured from the state of Perlis in Malaysia. As such, this present study used the impregnation method to synthesise Dol-supported Co and Cu monometallic and Co-Cu bimetallic catalysts. These three catalysts were used to conduct the hydrogenolysis of glycerol before multiple characterisation methods were used to analyse the correlations between their performance and properties. The impregnation method was used instead of the co-precipitation method as it is significantly easier to control the size of the metal particles in the catalyst (Karelovic & Ruiz, 2015).

MATERIALS AND METHODS

Chemicals

Perlis Dolomite Industries, Malaysia, supplied dolomite. Copper nitrate hexahydrate ($Cu(NO_3)_2.6H_2O$) ($\geq$ 99%) and cobalt nitrate hexahydrate ($Co(NO_3)_2.6H_2O$) ($\geq$99%) were purchased from R&M Chemical Company, Malaysia. Glycerol ($\geq$99.5%) was acquired from Sigma-Aldrich. The chemicals were used without further purification.

Catalyst Preparation

Every catalyst was synthesised using the impregnation procedure. The Co and Cu loading concentrations were set at 20 wt%. During the standard synthesis mechanism, copper nitrate ($Cu(NO_3)_2$, 3.8 g) and cobalt nitrate ($Co(NO_3)_2$, 4.9 g) were individually dissolved in distilled water (10 ml) and added to Dol powder (4 g) to produce Solution 1. A magnetic stirrer was used to stir the solution at 300 rpm before transferring it to a hot plate and left to dry at 90°C for 3 hours. It was then transferred to drying over to further age for 24 hours at 120°C. The catalyst was placed in a tube furnace to be calcined for 3 hours at 500°C with a temperature ramp rate of 10°C/min and static airflow to eliminate nitrate salt. Without removing the catalyst from the tube furnace, a 5% hydrogen/argon (H_2/Ar) gas mixture was then used to reduce it for 3 hours at 600°C and a temperature ramp rate of 2°C/min. The two catalysts produced were labelled "Cu/Dol" and "Co/Dol" for future use. A similar method was used to prepare the bimetallic catalyst by adding 20 wt% of the respective metal precursors to Solution 1, which was then stirred, dried, aged, calcined, and reduced. The bimetallic catalyst produced was labelled "Co-Cu/Dol". The performance of all three synthesised catalysts was examined by using them to conduct the hydrogenolysis of glycerol.

Catalyst Characterisation

A Micromeritics ® accelerated surface area and porosimetry (ASAP) 2010 system was used to observe the isotherms of nitrogen (N_2) adsorption-desorption of the synthesised catalysts and determine their textural characteristics (pore diameter, BET surface area, and

pore size) while their crystallite sizes and the structure of their phase compositions were determined by analysing their X-ray diffraction (XRD). Meanwhile, a Thermo-Finnigan® 1100 series TPDRO analyser equipped with a thermal conductivity detector (TCD) was used to observe their H_2-TPR and assess their metal reducibility as well as evaluate their distribution of acid sites and total acidity. Lastly, a Shimadzu® RayNy™ energy dispersive X-ray (EDX)-720 spectrometer was used to conduct SEM and examine their morphological characteristics. The analysis conducted in this present study has already been explained in great detail in our previous study (Azri et al., 2020).

Experimental Setup

The performance of the synthesised catalysts for the hydrogenolysis of glycerol was tested in a 150 mL capacity stainless steel (SS-316L) autoclave reactor and was explained in our previous study (Azri et al., 2020). Figure 1 depicts a schematic layout of the reactor setup used to examine the reactions.
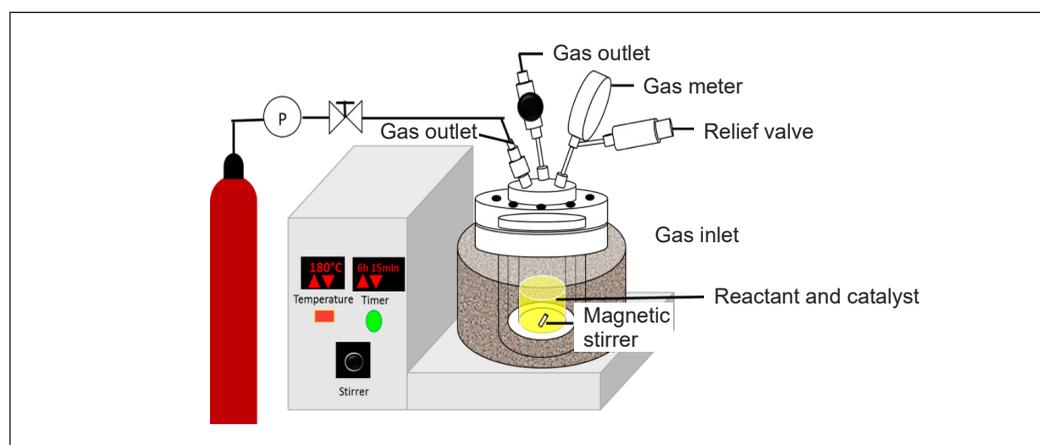

Figure 1. The experimental setup for glycerol hydrogenolysis reaction

Product Analysis

A flame ionisation detector (FID) fitted with an HP-5 capillary column was used to conduct gas chromatography (GC) on the liquid output of the experiment after it had been extracted thrice using ethyl acetate. The analytical procedure was similar to that of our previous study (Azri et al., 2020).

RESULTS AND DISCUSSION

Catalyst Characterisation

Table 1 presents the textural characteristics of the Dol, Co/Dol, Cu/Dol, and Co-Cu/Dol catalysts, such as the pore diameter, Brunauer, Emmett, and Teller (BET) surface area, and

Norsahida Azri, Ramli Irmawati, Usman Idris Nda-Umar, Mohd Izham Saiman, Yun Hin Taufiq-Yap and Ghassan Abdulkareem-Alsultan

pore size. The bimetallic catalyst showed an increase in the BET surface area to 21.9 m² g⁻¹ from the 13.3 m² g⁻¹ of the Dol. On the other hand, the surface area of the 20% Cu/Dol catalyst and 20% Ni/Dol catalyst showed a decrease to 9.7 m² g⁻¹ and 3.5 m² g⁻¹, respectively. These results could be attributed to the fact that the metal ions were filling the pores of the Dol support. Thirupathi et al. (2012) presented a similar finding and observed that the decreased surface area of the study's 0.4 manganese-nickel (Mn–Ni) and titanium dioxide (TiO_2) catalyst could be due to the nickel oxide (NiO) ions that were loaded onto the support material. The BET surface area showed the following trend: Co-Cu/Dol > Dol > Cu/Dol > Co/Dol.

In terms of pore volume, all Dol-supported catalysts have a smaller pore volume than Dol (0.276 cm³ g⁻¹). According to Zhao et al. (2013), this occurs because the metal species embeds and clogs the Dol matrix that covers the pores of the catalyst. The pore sizes of all Dol-supported catalysts (6.15 Å) were, similarly, smaller than that of Dol (156.34 Å). It is noteworthy that both the diameter and volume of the pores of the bimetallic catalyst were small. It may be attributed to the presence of fresh active sites or new pores on the surface of the bimetallic catalyst. During a catalytic reaction, the active sites on the surface of a catalyst initially adsorb or react before they move into the pores of the catalyst. However, in this case, the small pores of the catalyst may prevent leaching from occurring easily at the active sites, increasing the amount of adsorption-desorption that occurs there throughout the catalytic reaction. Furthermore, the active sites within the tiny pores may be beneficial when determining the reusability of a catalyst. It may also preserve the catalyst's stability throughout the subsequent cycle of reactions.

According to the IUPAC classification system, the isotherms of the N_2 adsorption-desorption, seen in Figure 2A, indicate that the synthesised catalysts had type III isotherms typical of macro-porous solids. The weak adsorption-desorption interaction between

Table 1
*Physicochemical properties of the catalysts*

Catalyst	BET		XRD		H₂-TPR			NH₃-TPD
	Surface area (m² g⁻¹)	Pore volume (cm³ g⁻¹)	Pore diameter (Å)	Crystallite size (nm)ᵃ	H₂ consumed at different temp (µmol/g)		Total amount H₂ consumed (µmol/g)	Total amount NH₃ adsorbed (µmol/g)
					150-550°C	> 550°C		> 550°C
Dolomite	13.3	0.276	152.02	27.4	-	1005	1005	16149
Cu/Dol	9.7	0.098	19.07	54.8	23582, 17919	10268	51769	19528
Co/Dol	7.8	0.145	156.34	22.9	19250	54712	73962	11172
Co-Cu/Dol	15.3	0.032	6.15	72.3	3719	1705	5424	11724

Note. ᵃ The data were estimated according to the Debye Scherrer equation using the FWHM of the dolomite peak at 2θ = 62°

adsorbed and desorbed molecules from the clustered solid catalyst was responsible for the isotherm results. Furthermore, similarities between the isotherms of the metal-supported catalysts and Dol indicate that the addition of metal ions did not significantly alter the structure of the Dol. As hysteresis developed in all the synthesised catalysts when the


(A)

(B)
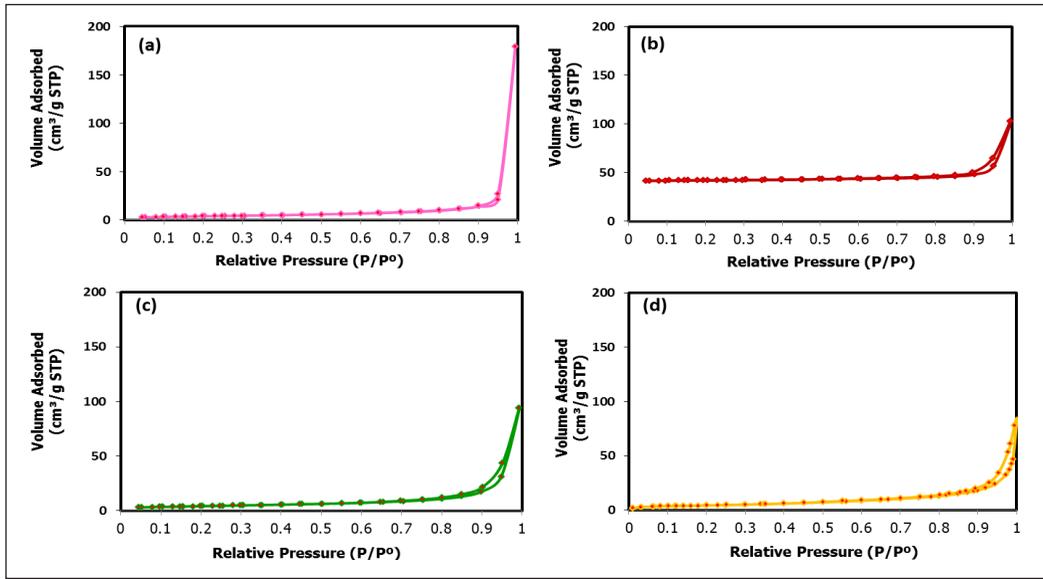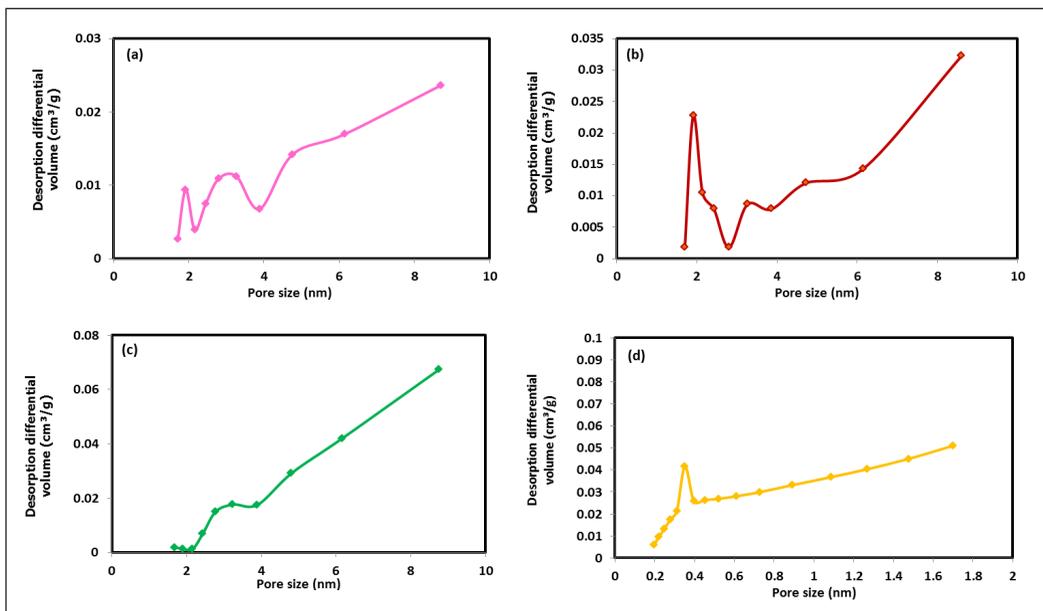
Figure 2. N$_2$-physisorption isotherms (A) and pore size distribution (B) of (a) Dolomite, (b) Cu/Dol, (c) Co/Dol, and (d) Co-Cu/Dol catalyst

relative pressure (p/p°) exceeded 0.8, their aggregates had the non-rigid characteristics of plate-shaped particles and a non-uniform size (Luna et al., 2018). It is commonly attributed to the capillary or delayed condensation capabilities of solid catalysts, as their multilayer pore network causes weak adsorption (Lopez et al., 2019). As all the synthesised catalysts, except the Cu/Dol catalyst, adsorbed little N_2 (~1 $cm^3 g^{-1}$), it underscored that the macro-porosity of the Cu/Dol catalyst was that of a solid catalyst. The Cu/Dol catalyst may have adsorbed more N_2 as its structure certain mesopores. The Barrett, Joyner, and Halenda (BJH) method was used to determine the curves of the pore size distributions of all the catalysts (Figure 2B). The distributions of the pore sizes of the Dol, Co/Dol, and Cu/Dol catalysts ranged between 2 to 10 nm, while that of the bimetallic Co-Cu/Dol catalyst was less than 2 nm.

Figure 3A depicts the XRD patterns of the calcined catalysts, while Figure 3B shows those of the reduced catalysts. Diffraction peaks in the Dol support were identified with heterogeneous crystalline phases. The peaks observed at $2\theta =18.1°$, $28.3°$ and $33.8°$ were attributed to the calcium-magnesium (1:2) phase ($CaMg_2$, Joint Committee on Powder Diffraction Standards (JCPDS) 01-1070) and the peaks observed at $2\theta = 37.51°$, $50.76°$, and $62.20°$ were attributed to the phase of the Dol (JCPDS 02-0767). Furthermore, the two peaks observed at $2\theta = 44.2°$ and $47.4°$ were attributed to the phase of $MgCO_3$ (JCPDS 02-0871). The peaks observed at $2\theta = 32.4°$ and $54.2°$ were attributed to the calcium oxide (CaO) phase (JCPDS 01-1160), and the lower intensity peak observed at $2\theta = 78.7°$ was attributed to the magnesium aluminate ($MgAl_2O_4$) phase (JCPDS 03-1160).

With regards to the monometallic and bimetallic catalysts, the XRD patterns indicated that the novel phases corresponded to the corresponding metal oxide molecules as the metal oxide species had become embedded in the matrix of the Dol support; more specifically, copper oxide (CuO) at $2\theta = 35.5°$ and $38.8°$ (JCPDS 44-0706) and cobalt carbonate ($CoCO_3$) at $2\theta = 33.5°$ (JCPDS 01-1020). Alloy phases were also observed in the bimetallic catalysts; more specifically, the güggenite (Cu_2MgO_3) phase at $2\theta = 48°$ (JCPDS 21-0291) and the cobalt-magnesium (2:1) (Co_2Mg) phase at $2\theta = 42°$, $44.5°$, $74.5°$ and $76°$ (JCPDS 29-0486). Extant studies have similarly concluded that metal oxide species are more likely to produce spinel when supported by limestone or clay materials containing Mg and Ca ions (Kovanda et al., 2001; Pardeshi et al., 2010). However, the calcined catalysts did not show the presence of any peaks that correlate with metallic species.

As seen in Figure 3B, the CuO diffraction peaks ($2\theta = 35.5°$ and $38.8°$) had vanished, whereas the peaks of the Cu ($2\theta = 43.5°$ and $74.3°$) (JCPDS; 085-1326), which is metallic, appeared in the bimetallic and monometallic catalysts. The metallic copper (Cu^0) species may have appeared due to the effective transfer of electrons between the oxide species and the Dol support, which would destabilise the bonds of the metal oxide and help reduce the metal species. The interfacial sites of the metal-support material helped coordinate
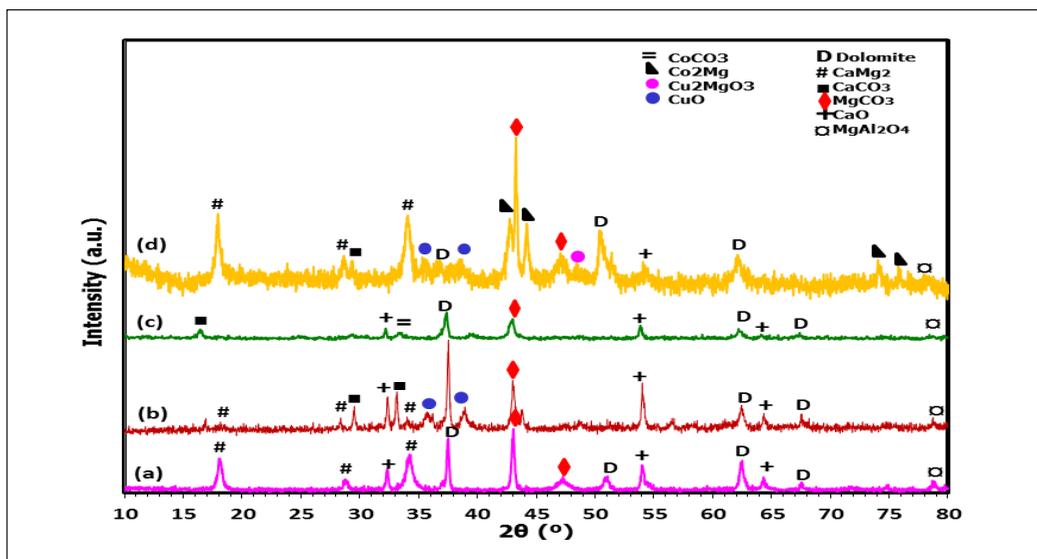
(A)
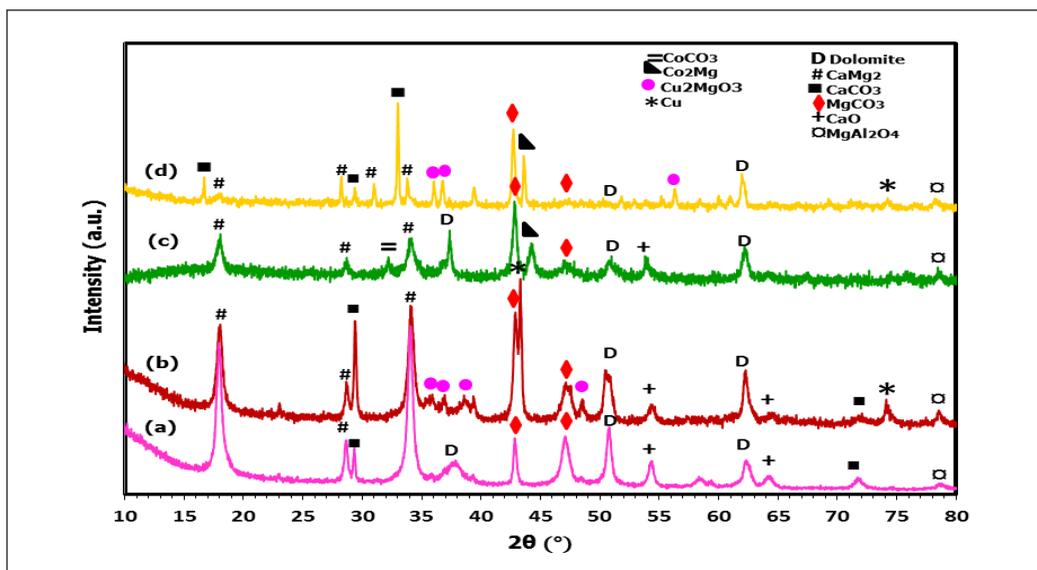
(B)

Figure 3. XRD diffractograms of calcined (A) and reduced samples (B) of (a) Dolomite, (b) Cu/Dol, (c) Co/Dol, and (d) Co-Cu/Dol catalyst

the oxygen atoms with the help of a single pair of electrons, which facilitates electron migration and helps reduce the metal oxide species (Nagaraja et al., 2007). As Ca and Mg are good reducers, this study hypothesised that the $CaMg(CO_3)_2$, CaO, and $MgCO_3$ surface species of the Dol reduced the metal oxide (Tasyurek et al., 2018). Furthermore, the peak of the Co_2Mg phase was observed at $2\theta = 44.5^o$, while those of the Cu_2MgO_3 phase were

observed at $2\theta = 35.3°$, $37.5°$, $38.2°$, and $48°$. However, the reduced catalysts did not present any characteristic peak associated with the Co and Cu oxide species.

As seen in Table 1, the crystallites of the bimetallic catalyst were larger than those of the monometallic catalysts. Therefore, the higher concentration of metal oxide, which increased the amount of intercalated Cu and Co in the catalyst, caused the metal species to fill the interstitial spaces of the Dol bulk and increased the size of the crystallites. The crystallite sizes were, in descending order, Co-Cu/Dol > Cu/Dol > Co/Dol. The higher intensity non-shifting peaks of $MgCO_3$ observed at $2\theta = 47.4°$ and $43.5°$ in the Dol indicate the increase in the size of the crystallites. The non-shifting characteristic of the peaks also indicates that the metal species had incorporated into the support well (Asikin-Mijan et al., 2017). The size of the particles of a catalyst may directly affect H_2 adsorption or activation and hydrogenation, especially during the hydrogenolysis of glycerol.

Figure 4 depicts all the catalysts' H_2-TPR profiles, while Table 1 lists their H_2 adsorption. The reduction profiles indicate that incorporating Cu and/or Co species into the Dol caused reduction peaks that were lower than that of the Dol to appear. The reduction peaks observed at 291 and 455°C, 444°C only, and 277 and 435°C were attributed to the Cu/Dol, Co/Dol, and bimetallic catalysts, respectively. The appearance of a reduction peak at low temperatures indicates weakly bonded or dispersed metal oxide species (species). In contrast, the appearance of a reduction peak at temperatures that exceed 400°C indicates the reduction of metal oxides as a complex species as a consequence of increased interactions between the metals and the support material (Shozi et al., 2017; Wen et al., 2013; Zhao et al., 2017). The presence of Cu in the aluminate spinel ($CuAl_2O_4$) and complex Cu phases of $Cu_xMg_xAl_2O_4$ led to the reduction of the mixed oxides that contained Cu at 400 to 750°C (Tanasoi et al., 2009). This present study observed the two peaks at 277 and 291°C, which could be attributed to the dispersed CuO species reducing to Cu^0. On the other hand, the peak observed between 435 to 455°C was attributed to the Cu or Co species-containing mixed oxides reducing (Tanasoi et al., 2009; Vargas-Hernández et al., 2014).

As Cu_2MgO_3 and Co_2Mg peaks were observed in the XRD pattern, the results of this present study could be attributed to the Co and Cu oxides reducing the defects present in the interstitial spaces of the Dol phase. The peaks observed at 616 to 638°C were attributed to the Dol reducing as they were similar to that of a Dol bulk (639°C) (Azri et al., 2020). Furthermore, compared to the monometallic catalysts, the reduction of the bimetallic catalyst effectively shifted toward the lower temperatures (277°C). It was attributed to significant interactions between the Co-Cu-Dol species of the bimetallic catalyst, which enhanced and altered its metal reducibility. However, the reduction peaks observed at 638°C in the Co/Dol catalyst were broader and higher than that of the Dol peak. It may be due to the reduction of the Co species, which significantly interacted with the Dol support and is also supported by the findings of the XRD analysis, which detects the $CoCO_3$

species. Extant studies have similarly concluded that taller and wider peaks appear when strong metal-support species reduce as it requires more H_2 adsorption, which broadens the reduction peak (Li et al., 2009). The interphase H_2 adsorption or the slow diffusion of the hydrogen ions in a thoroughly sintered metal species may also cause a wider reduction peak (Soares et al., 2016).

As seen in Table 1, the Dol adsorbed less total H_2 than the monometallic and bimetallic catalysts. Extant studies have similarly found that a catalyst containing CuO and ceric oxide (CeO_2) adsorbed significantly more H_2 than required to completely reduce unadulterated CuO (Zhao et al., 2019). Therefore, the Ce may have played a role in the reduction. It suggests that metal species with larger exposure areas are more reducible but increase the H_2 consumption of the catalyst. The monometallic and bimetallic catalysts had wider and taller reduction peaks than the Dol as they adsorbed more H_2. Furthermore, it was advantageous that the metal species were reduced to under 300°C as the metallic species remained stable and active throughout the catalytic reaction process, which occurred at 200°C. It would significantly improve H_2 adsorption on the surface of the catalyst and expedite the hydrogenolysis reaction. As alloy instead of metallic species appeared in the monometallic and bimetallic catalysts, the presence and reduction of CaO, $MgCO_3$, $CaCO_3$, and $MgAl_2O_4$ phases of the Dol warrant further investigation as a source of chemisorption in H_2 atoms and higher H_2 uptake.

Acid sites are required to activate the C-O bonds of glycerol molecules through dehydration (Zhu et al., 2013). The NH_3 adsorption and dissociation ability of a catalyst can be used to determine its acidity. Acid strengths are classified as weak if they remain below 250°C, medium between 250 to 500°C, and strong if they exceed 500°C (Srivastava
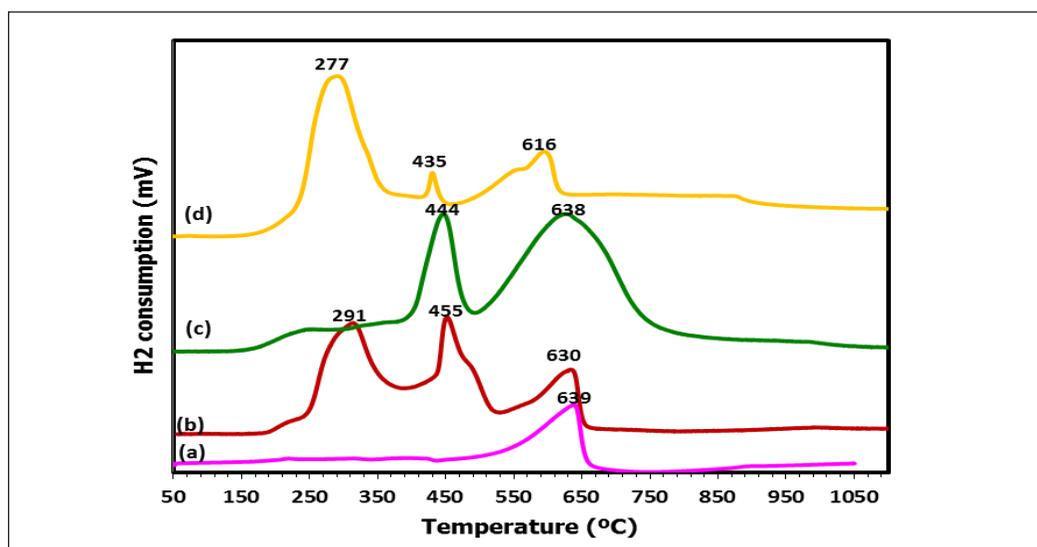

Figure 4. H_2-TPR profiles of (a) Dolomite, (b) Cu/Dol, (c) Co/Dol, and (d) Co-Cu/Dol catalyst

et al., 2017). Figure 5 displays the NH_3 desorption profiles of the three synthesised catalysts, whereas Table 1 presents their acidity data, which is the concentration of ammonia absorption. All three catalysts contained significant acid sites, with desorption peaks that exceeded 500°C. More specifically, the desorption peaks of the Dol were observed at 805 and 874°C, that of the Cu/Dol catalyst at 718 and 948°C, and that of the Co/Dol catalyst at 712 and 815°C while the bimetallic catalyst had the lowest desorption peak (589°C). Stronger acid sites were present on the surface of the catalyst, as evidenced by the high desorption temperature of the Cu/Dol catalyst (948°C) over the Dol. It matched the total NH_3 desorption amount (Table 1).

The Cu/Dol catalyst had the highest acidity of all three catalysts. As such, the acidity of the catalysts was, in descending order, Cu/Dol > Dol > Co-Cu/Dol > Co/Dol. As the Co-Cu/Dol and Co/Dol catalysts were less acidic than the Dol, the metal species in the Dol may have encased and blocked its surface, thereby limiting the amount of NH_3 it desorbed (Priya et al., 2017). The decreased acidity with loading of Co-Cu can also be attributed to increased agglomeration on the surface of the catalyst upon incorporation of the metals, thereby hindering the surface from absorption of ammonia into catalyst pores, leading to decreased pore volume and diameter as indicated in Table 1. The acidity of the catalysts may also be due to the $MgCO_3$ and $CaCO_3$ phases of the Dol (Azri et al., 2020).

Figure 6 depicts the SEM-based surface morphology of the catalysts. The SEM photomicrographs showed that all the catalysts contained irregular agglomerated structures that measured 10 mm on average on a scale bar. Therefore, the macro-porous solids had formed tightly clustered crystals.

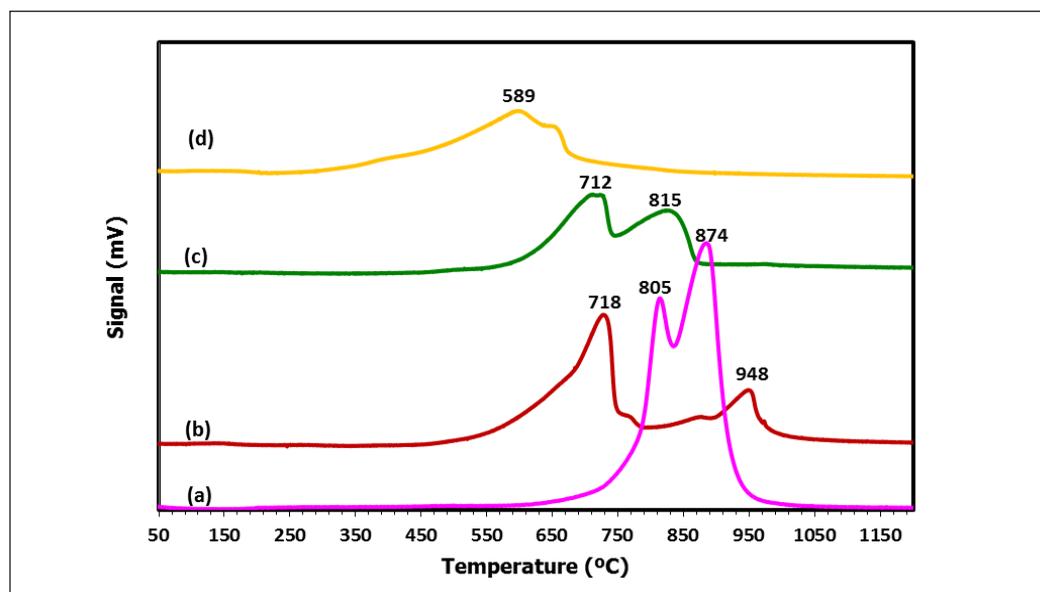*Figure 5.* NH_3-TPD profiles of (a) Dolomite, (b) Cu/Dol, (c) Co/Dol, and (d) Co-Cu/Dol catalyst
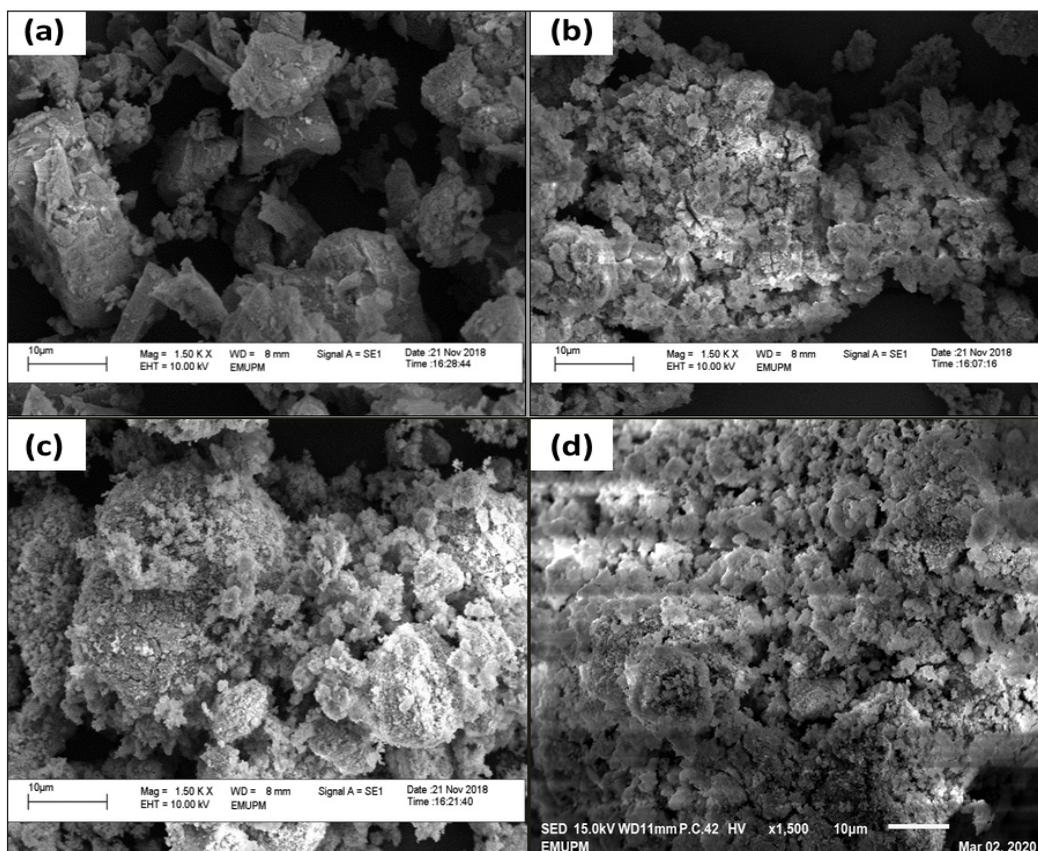
Figure 6. SEM images of (a) Dolomite, (b) Cu/Dol, (c) Co/Dol, and (d) Co-Cu/Dol catalyst

Catalytic Activity

Table 2 presents the catalytic activities of glycerol hydrogenolysis using each catalyst. A blank reaction or control experiment was also carried out, which meant conducting the hydrogenolysis sans a catalyst and/or support. The conversion of glycerol and selectivity of PG, acetol, and methanol were used to evaluate the performance of each catalyst. Without a catalyst and/or support, the control experiment could only convert 8.7% of the glycerol and did not select the PG. The introduction of a catalyst had a profound impact. Although the Dol was able to convert 10.6% of the glycerol, it lacked selectivity for PG.

Therefore, the Dol could not catalyse glycerol to PG hydrogenolysis on its own. The catalytic reaction was significantly influenced by adding metal ions to the Dol. The bimetallic Co-Cu/Dol catalyst outperformed the other catalysts in terms of glycerol conversion (80.3%) and PG selectivity (85.9%). Its elevated turnover frequency (TOF) also confirmed its significant catalytic activity. Compared to the bimetallic catalyst, the glycerol conversion and PG selectivity of the monometallic catalysts were poorer; more specifically, 78.5% and 79% for the Cu/Dol catalyst and 60.9% and 58.1% for the Co/Dol

Table 2
Performance of the synthesised catalysts

Sample	Conversion (%)	Selectivity (%)			TOF (h^{-1})
		Acetol	1,2-PDO	Methanol	
Blank	8.7	0	0	0	-
Dolomite	10.6	6.3	0	93.7	0.46
Cu/Dol	78.5	18.9	79	2.1	3.41
Co/Dol	60.9	14.2	58.1	27.6	2.65
Co-Cu/Dol	80.3	4.3	85.9	9.9	3.49

Note. Reaction conditions: 20 ml of aqueous glycerol (20wt%); reaction temperature 200 ºC; H$_2$ pressure 4 MPa; catalyst dosage 1g; reaction time 10 hr

catalyst, respectively. Therefore, the glycerol hydrogenolysis performance of the catalysts was, in descending order, Co-Cu/Dol > Cu/Dol > Co/Dol > Dol. It also proves that the inclusion of Co and Cu in Dol increases its glycerol conversion and PG selectivity.

The bimetallic catalyst outperformed the other catalysts, potentially, because it possessed adequate acidity (11724 µmol/g), a high surface area (15.3 m^{2}g^{-1}), fewer pores (0.032 cm^{3}g^{-1}), and smaller pores (0.615 nm). The presence of sufficient surface acid sites aided in the dehydration of the glycerol molecules to generate acetol, which resulted in PG. Extant studies indicate that acid sites significantly affect hydrogenolysis (Putrakumar et al., 2015; Yuan et al., 2009). Metallic sites on the surface of a catalyst are also essential as they enable hydrogenation to occur by breaking H$_2$ down to hydride, which helps hydrogenate the intermediate acetol to PG. The catalytic performance of a bimetallic catalyst correlates to the presence of Cu metallic species. The results of this present study demonstrate that the presence of bifunctional sites on the bimetallic catalysts led to the simultaneous and rapid dehydration of glycerol to acetol and the hydrogenation of acetol to PG, as also proposed in the literature (Scheme 1).
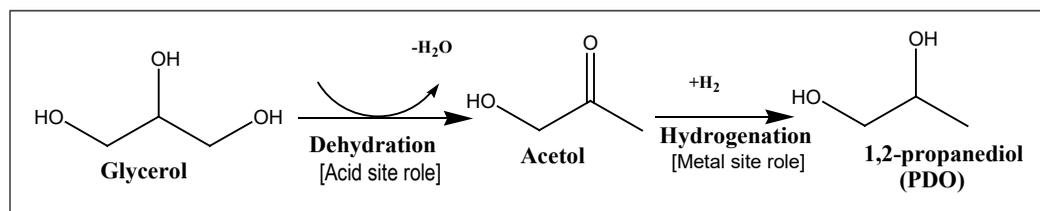
Scheme 1. Glycerol hydrogenolysis pathway over metal-acid condition (Mallesham et al., 2016)

However, H$_2$ adsorption or activation may determine if a hydrogenation reaction is high or low, as H$_2$ supplies the hydride required to hydrogenate the intermediate product during a catalytic reaction. The ability of a catalyst to adsorb high amounts of H$_2$ may correlate with the size of its metal particles. Extant studies have similarly indicated a linear correlation between the catalytic activity and the H$_2$ adsorption of catalysts with large-sized

metal particles (Karelovic & Ruiz, 2015). Catalysts with large-sized metal particles have larger surface areas and interfacial exposure, which improves H_2 adsorption as more H_2 can be activated on the surface of the catalyst, and there is better accessibility to metallic reaction sites. In turn, it significantly encourages the cleaving of the C-O bond during hydrogenation.

As seen in Table 1, the crystallite particle sizes of the bimetallic catalyst were larger than those of the other catalysts, which may have facilitated its high PG selectivity. Hydrogen (H_2) adsorption is believed to be more active in large-sized metal particles as the surface exposure of the metal is larger. Therefore, more H_2 can be activated on the surface of the catalyst. It also increases accessibility to metallic sites, which, in turn, increases its reactivity towards the C-O bonds *via* hydrogenation, which increases the amount of PG produced. Conversely, the smaller particle sizes of the monometallic catalysts decreased their PG selectivity.

The results reveal that the bimetallic catalyst had better catalytic performance than the monometallic catalysts. The catalytic efficiency of the bimetallic Co-Cu/Dol catalysts could have been influenced by different factors such as appropriate acidity, large particle size, good metal reducibility, high surface area, fewer pores, and smaller pore diameters. The bimetallic catalyst had good glycerol conversion and PG selectivity when factors such as pressure, reaction temperature, and reaction duration were optimised, in comparison to the results of extant studies (Table 3).

Table 3
Comparison of the result obtained in this work with other results from the literature

Catalyst	Reaction parameters				Conv (%)	Sel (%)	References
	Temp (ºC)	H_2 (MPa)	Time (h)	Cat Dosage (g)		1,2-PDO	
$Cu-Ni/Al_2O_3$	210	4.5	12	2	60	89	Pudi et al., 2015
$Cu/Ce/Mg$	200	6	10	1	56.4	97.4	Mallesham et al., 2016
$Cu-Ni/Al_2O_3$	220	4.5	16	0.9	70.5	70	Gandarias et al., 2012
$Ru–Cu/Al_2O_3$	200	2.5	24	2	45	94	Soares et al.,2016
$Ru–Cu/ZrO_2$	200	2.5	24	2	13.7	100	Soares et al.,2016
$Ni–Co/Al_2O_3$	220	6	10	2	63.5	60.4	Jiang et al., 2016
$Ni-Co/Ce$	220	6	10	2	71.3	68.5	Jiang et al., 2016
$Ni-Cu/Dol$ [a]	200	4	10	1	80	88.4	Present work

CONCLUSION

The bimetallic Co-Cu/Dol catalyst that this present study proposed had a maximum glycerol conversion of 80.3% and a maximum PG selectivity of 85.9% at a reaction temperature of 200ºC, reaction pressure of 4 MPa, and a reaction duration of 10 hours. It performed the best as it had effective Cu-Co-Dol interactions, an optimal acidity of 11724 µmol/g,

a large surface area of $15.3 \ m^2 \, g^{-1}$, a good ability to reduce metal oxide species at a low temperature of 277°C, a pore diameter of 0.615 nm, fewer pores ($0.032 \ cm^3 \, g^{-1}$), and large particle sizes (72.3 nm).

ACKNOWLEDGEMENTS

REFERENCES

Asikin-Mijan, N., Lee, H. V., Juan, J. C., Noorsaadah, A. R., & Taufiq-Yap, Y. H. (2017). Catalytic deoxygenation of triglycerides to green diesel over modified CaO-based catalysts. *RSC Advances, 7*(73), 46445-46460. https://doi.org/10.1039/C7RA08061A

Azri, N., Ramli, I., Nda-Umar, U. I., Shamsuddin, M. Razali., Saiman, M. I., & Taufiq-Yap, Y. H. (2020). Copper-dolomite as effective catalyst for glycerol hydrogenolysis to 1,2-propanediol. *Journal of the Taiwan Institute of Chemical Engineers, 112,* 34-51. https://doi.org/10.1016/j.jtice.2020.07.011

Bagheri, S., Muhd, N., & Yehye, W. A. (2015). Catalytic conversion of biodiesel derived raw glycerol to value added products. *Renewable and Sustainable Energy Reviews, 41*, 113-127. https://doi.org/10.1016/j.rser.2014.08.031

Feng, Y., Yin, H., Wang, A., Shen, L., Yu, L., & Jiang, T. (2011). Gas phase hydrogenolysis of glycerol catalyzed by $Cu/ZnO/MO_x$ (MO_x = Al_2O_3, TiO_2, and ZrO_2) catalysts. *Chemical Engineering Journal, 168*(1), 403–412. https://doi.org/10.1016/j.cej.2011.01.049

Freitas, I. C., Manfro, R. L., & Souza, M. M. V. M. (2018). Hydrogenolysis of glycerol to propylene glycol in continuous system without hydrogen addition over Cu-Ni catalysts. *Applied Catalysis B: Environmental, 220*, 31–41. https://doi.org/10.1016/j.apcatb.2017.08.030

Gallegos-Suarez, E., Guerrero-Ruiz, A., Rodriguez-Ramos, I., & Arcoya, A. (2015). Comparative study of the hydrogenolysis of glycerol over Ru-based catalysts supported on activated carbon, graphite, carbon nanotubes and KL-zeolite. *Chemical Engineering Journal, 262*, 326–333. https://doi.org/10.1016/j.cej.2014.09.121

Gandarias, I., Requies, J., Arias, P. L., Armbruster, U., & Martin, A. (2012). Liquid-phase glycerol hydrogenolysis by formic acid over $Ni–Cu/Al_2O_3$ catalysts. *Journal of Catalysis, 290*, 79–89. https://doi.org/10.1016/j.jcat.2012.03.004

Guo, X., Li, Y., Shi, R., Liu, Q., Zhan, E., & Shen, W. (2009). Co/MgO catalysts for hydrogenolysis of glycerol to 1, 2-propanediol. *Applied Catalysis A: General, 371*(1-2), 108–113. https://doi.org/10.1016/j.apcata.2009.09.037

Jiang, T., Kong, D., Xu, K., & Cao, F. (2016). Hydrogenolysis of glycerol aqueous solution to glycols over Ni–Co bimetallic catalyst: Effect of ceria promoting. *Applied Petrochemical Research, 6*, 135–144. https://doi.org/10.1007/s13203-015-0128-8

Karelovic, A., & Ruiz, P. (2015). The role of copper particle size in low pressure methanol synthesis via CO_2 hydrogenation over Cu/ZnO catalysts. *Catalysis Science & Technology, 5*(2), 869–881. https://doi.org/10.1039/C4CY00848K

Kovanda, F., Jiratova, K., Rymes, J., & Kolousek, D. (2001). Characterization of activated Cu/Mg/Al hydrotalcites and their catalytic activity in toluene combustion. *Applied Clay Science, 18*(1-2), 71-80. https://doi.org/10.1016/S0169-1317(00)00032-6

Li, Y., Guo, Y., & Xue, B. (2009). Catalytic combustion of methane over M (Ni, Co, Cu) supported on ceria-magnesia. *Fuel Processing Technology, 90*(5), 652-656. https://doi.org/10.1016/j.fuproc.2008.12.002

Liu, Y., Guo, X., Rempel, G. L., & Ng, F. T. T. (2019). The promoting effect of *Ni* on glycerol hydrogenolysis to 1,2propanediol with in situ hydrogen from methanol steam reforming using a $Cu/ZnO/Al_2O_3$ catalyst. *Catalysts, 9*(5), Article 412. https://doi.org/10.3390/catal9050412

Luna, F. M. T., Cecilia, J. A., Saboya, R. M. A., Barrera, D., Sapag, K., Rodríguez-Castellón, E., & Jr, C. C. L. (2018). Natural and modified montmorillonite clays as catalysts for synthesis of biolubricants. *Materials, 11*(9), Article 1764. https://doi.org/10.3390/ma11091764

Lopez, A., Aragon, J. A., Hernandez-Cortez, J. G., Mosqueira, M. L., & Martinez-Palou, R. (2019). Study of hydrotalcite-supported transition metals as catalysts for crude glycerol hydrogenolysis. *Molecular Catalysis, 468*, 9–18. https://doi.org/10.1016/j.mcat.2019.02.008

Mallesham, B., Sudarsanam, P., Reddy, B. V. S., & Reddy, B. M. (2016). Development of cerium promoted copper–magnesium catalysts for biomass valorization: Selective hydrogenolysis of bioglycerol. *Applied Catalysis B: Environmental, 181*, 47–57. https://doi.org/10.1016/j.apcatb.2015.07.037

Nagaraja, B. M., Padmasri, A. H., Seetharamulu, P., Reddy, K. H. P., Raju, B. D., & Rao, K. R. (2007). A highly active $Cu-MgO-Cr_2O_3$ catalyst for simultaneous synthesis of furfuryl alcohol and cyclohexanone by a novel coupling route-Combination of furfural hydrogenation and cyclohexanol dehydrogenation. *Journal of Molecular Catalysis A: Chemical, 278*(1-2), 29-37. https://doi.org/10.1016/j.molcata.2007.07.045

Pandhare, N. N.,Pudi, S. M., Biswas, P., & Sinha, S. (2016). Vapor phase hydrogenolysis of glycerol to 1, 2-propanediol over γ-Al_2O_3 supported copper or nickel monometallic and copper–nickel bimetallic catalysts. *Journal of the Taiwan Institute of Chemical Engineers, 61*, 90–96. https://doi.org/10.1016/j.jtice.2015.12.028

Pardeshi, S. K., & Pawar, R. Y. (2010). Optimization of reaction conditions in selective oxidation of styrene over fine crystallite spinel-type $CaFe_2O_4$ complex oxide catalyst. *Materials Research Bulletin, 45*(5), 609-615. https://doi.org/10.1016/j.materresbull.2010.01.011

Priya, S. S., Selvakannana, Komandur, P. R., Chary, V. R., Kantam, M. L., & Bhargava, S. K. (2017). Solvent-free microwave-assisted synthesis of solketal from glycerolusing transition metal ions promoted mordenite solid acid catalysts. *Molecular Catalysis, 434*, 184–193. https://doi.org/10.1016/j.mcat.2017.03.001

Pudi, S. M., Biswas, P., Kumar, S., & Sarkar, B. (2015). Selective hydrogenolysis of glycerol to 1,2 propanediol over bimetallic Cu-Ni catalysts supported on γ-Al_2O_3. *Journal of the Brazilian Chemical Society, 26*(8), 1551–1564. https://doi.org/10.5935/0103-5053.20150123

Putrakumar, B., Nagaraju, N., Kumar, V. P., & Chary, K. V. R. (2015). Hydrogenation of levulinic acid to valerolactone over copper catalysts supported on Al_2O_3. *Catalysis Today, 250*, 209–217. https://doi.org/10.1016/j.cattod.2014.07.014

Rajkhowa, T., Marin, G. B., & Thybaut. J. W. (2017). A comprehensive kinetic model for Cu catalyzed liquid phase glycerol hydrogenolysis. *Applied Catalysis B: Environmental*, *205*, 469– 480. https://doi.org/10.1016/j.apcatb.2016.12.042

Shozi, M. L., Dasireddy, V. D. B. C., Singh, S., Mohlala, P., Morgan, D. J., Iqbal, S., & Friedrich, H. B. (2017). An investigation of Cu–Re–ZnO catalysts for the hydrogenolysis of glycerol under continuous flow conditions. *Sustainable Energy & Fuels, 1*(6), 1437–1445. https://doi.org/10.1039/C7SE00199A

Soares, A. V., Perez, G., & Passos, F. B. (2016). Alumina supported bimetallic Pt–Fe catalysts applied to glycerol hydrogenolysis and aqueous phase reforming. *Applied Catalysis B: Environmental, 185*, 77–87. https://doi.org/10.1016/j.apcatb.2015.11.003

Soares, A. V. H., Salazar, J. B., Falcone, D. D., Vasconcellos, F. A., Davis, R. J., & Passos, F. B. (2016). A study of glycerol hydrogenolysis over Ru–Cu/Al_2O_3 and Ru–Cu/ZrO_2 catalysts. *Journal of Molecular Catalysis A: Chemical, 415*, 27–36. https://doi.org/10.1016/j.molcata.2016.01.027

Srivastava, S., Jadeja, G. C., & Parikh, J. (2017). Synergism studies on alumina-supported copper nickel catalysts towards furfural and 5-hydroxymethylfurfural hydrogenation. *Journal of Molecular Catalysis A: Chemical, 426*(Part A), 244–256. https://doi.org/10.1016/j.molcata.2016.11.023

Tanasoi, S., Tanchoux, N., Adriana, U., Tichit, D., Sandulescu, I., Fajula, F., & Marcu, I. C. (2009). New Cu-based mixed oxides obtained from LDH precursors, catalysts for methane total oxidation. *Applied Catalysis A: General, 363*(1-2), 135-142. https://doi.org/10.1016/j.apcata.2009.05.007

Tasyurek, K. C., Bugdayci, M., & Yucel, O. (2018). Reduction conditions of metallic calcium from magnesium production residues. *Metals, 8*(6), Article 383. https://doi.org/10.3390/met8060383

Thirupathi, B., & Smirniotis, P. G. (2012). Nickel-doped Mn/TiO_2 as an efficient catalyst for the low-temperature SCR of NO with NH_3: Catalytic evaluation and characterizations. *Journal of Catalysis, 288*, 74–83. https://doi.org/10.1016/j.jcat.2012.01.003

Vanama, P. K., Kumar, A., Ginjupalli, S. R., & Komandur, V. R. C. (2015). Vapor-phase hydrogenolysis of glycerol over nanostructured Ru/MCM-41 catalysts. *Catalysis Today, 250*, 226–238. https://doi.org/10.1016/j.cattod.2014.03.036

Vargas-Hernández, D., Rubio-Caballero, J. M., Santamaría-González, J., Moreno-Tost, R., Mérida-Robles, J. M., Pérez-Cruz, M. A., Jiménez-López, A., Hernández-Huesca, R., & Maireles-Torres, P. (2014). Furfuryl alcohol from furfural hydrogenation over copper supported on SBA-15 silica catalysts. *Journal of Molecular Catalysis A: Chemical, 383-384*, 106–113. https://doi.org/10.1016/j.molcata.2013.11.034

Vasiliadou, E. S., & Lemonidou, A. A. (2011). Investigating the performance and deactivation behaviour of silica-supported copper catalysts in glycerol hydrogenolysis. *Applied Catalysis A: General, 396*(1-2), 177-185. https://doi.org/10.1016/j.apcata.2011.02.014

Wen, C., Yin, A., Cui, Y., Yang, X., Dai, W. L., & Fan, K. (2013). Enhanced catalytic performance for SiO_2–TiO_2 binary oxide supported Cu-based catalyst in the hydrogenation of dimethyloxalate. *Applied Catalysis A: General, 458*, 82– 89. https://doi.org/10.1016/j.apcata.2013.03.021

Yu, W., Zhao, J., Ma, H., Miao, H., Song, Q., & Xu, J. (2010). Aqueous hydrogenolysis of glycerol over Ni–Ce/AC catalyst: Promoting effect of Ce on catalytic performance. *Applied Catalysis A: General, 383*(1-2), 73-78. https://doi.org/10.1016/j.apcata.2010.05.023

Yuan, Z., Wu, P., Gao, J., & Lu, X. (2009). Pt/solid-base: A predominant catalyst for glycerol hydrogenolysis in a base-free aqueous solution. *Catalysis Letters, 130,* 261-265. https://doi.org/10.1007/s10562-009-9879-0

Zhao, F., Li, S., Wu, X., Yue, R., Li, W., Zha, X., Deng, Y., & Chen, Y. (2019). Catalytic behaviour of flame-made CuO-CeO$_2$ nanocatalysts in efficient co oxidation. *Catalysts, 9*(3), Article 256. https://doi.org/10.3390/catal9030256

Zhao, S., Yue, H., Zhao, Y., Wang, B., Geng, Y., Lv, J., Wang, S., Gong, J., & Ma, X. (2013). Chemoselective synthesis of ethanol via hydrogenation of dimethyl oxalate on Cu/SiO$_2$: Enhanced stability with boron dopant. *Journal of Catalysis, 297*, 142-150. https://doi.org/10.1016/j.jcat.2012.10.004

Zhao, Y., Zhang, Y., Wang, Y., Zhang, J., Xu, Y., Wang, S., & Ma, X. (2017). Structural evolution of mesoporous silica supported copper catalyst for dimethyl oxalate hydrogenation. *Applied Catalysis A: General, 539*, 59–69. https://doi.org/10.1016/j.apcata.2017.04.001

Zheng, L., Xia, S., & Hou, Z. (2015). Hydrogenolysis of glycerol over Cu-substituted hydrocalumite mediated catalysts. *Applied Clay Science, 118*, 68–73. https://doi.org/10.1016/j.clay.2015.09.002

Zhu, S., Gao, X., Zhu, Y., Zhu, Y., Zheng, H., & Li, Y. (2013). Promoting effect of boron oxide on Cu/SiO$_2$ catalyst for glycerol hydrogenolysis to 1,2-propanediol. *Journal of Catalysis, 303*, 70–79. https://doi.org/10.1016/j.jcat.2013.03.018